Microchemical Journal 208 (2025) 112545

Contents lists available at ScienceDirect

Microchemical Journal

journal homepage: www.elsevier.com/locate/microc

Development of hydroxyapatite nanoparticles modified pencil graphite electrodes for voltammetric detection of paracetamol and phenol and greenness assessment of the sensor platform

Gulsah Congur [a,b,*], Elif Efe [b]

[a] Department of Pharmacy, Vocational School of Health Services, Bilecik Seyh Edebali University, 11100 Bilecik, Turkey
[b] Institute of Graduate Studies, Department of Biotechnology, Bilecik Seyh Edebali University, Bilecik, Turkey

ARTICLE INFO

Keywords:
Hydroxyapatite nanoparticles
Pencil graphite electrode
Phenol
Paracetamol
Voltammetric analysis
AGREE

ABSTRACT

Detection of phenolic compounds in water resources has a great importance since their monitoring is obligatory for the evaluation of water quality, and they are major contaminants in water. Phenol and high concentrations of phenolic compounds have serious side effects on both aquatic life and human health. Within the scope of this study, a novel disposable electrochemical sensor platform was fabricated to monitor of phenol (PNL) and an emerging phenolic contaminant, paracetamol (PRL). For this purpose, disposable pencil graphite electrodes (PGEs) were modified with hydroxyapatite nanoparticles (HaNP) following a novel method. First, the PGEs were chemically activated using NaOH (N-PGEs), and modified with HaNPs (HaNP/N-PGEs) in an acidic media to activate positive charges of HaNP. Then, the HaNP-N/PGEs were used for the voltammetric detection of PRL and PNL. The effect of the experimental parameters such as pH, scan rate and concentration of PRL or PNL were investigated using cyclic voltammetry (CV) technique. Lower LOD values could be obtained by using HaNP/N-PGEs in comparison to the N-PGEs due to the fact that enhanced electrochemically active surface area was obtained by the modification of HaNP on the PGE surface. Simultaneous detection of PRL and PNL was tested using differential pulse voltammetry (DPV) technique. The selectivity of the sensor was also evaluated in the presence of inorganic and organic compounds, and PRL and PNL detection was performed in drinking water and wastewater samples. The greennness level of the sensor was evaluated using Analytical GREEnness Metric Approach and Software (AGREE). This is the first study in the literature in terms of (i) the development of HaNP/N-PGEs, (ii) voltammetric PRL/PNL detection using HaNP/N-PGEs, and (iii) greenness assessment of a PGE-based electrochemical sensor. The HaNP/N-PGEs based electrochemical sensor platform represents a novel and green prototype towards future hand-held devices for reliable monitoring of phenolic compounds.

1. Introduction

Our world is on the verge of water scarcity crisis. Global population has raised day-by-day and we should protect our limited natural resources on our one and only home, Earth. Although almost everyone is aware of global warming, industrial activities has not stopped, wars have been expanding their territories and have become more and more severe, global forest fires have suddenly arised due to high temperatures and dry air. Unfortunately, most of the population has directly been affected from all of these situations, and serious actions should be taken for the protection of water sources.

Phenol (PNL) is a major contaminant found in the water resources both naturally and as a by-product of industrial activities. PNL and phenolic compounds are highly toxic, harmful for environment and human health, and most of them are found in water resources [1,2]. Therefore, the development of analytical platforms for the monitoring of PNL and phenolic compounds is an attractive topic for researchers. Paracetamol (PRL) is one of the water-soluble phenolic compound widely used as a medication for treatment of fever and headache [3,4]. Its uncontrolled use has mostly occurred during the pandemic period and has caused water resources to be contaminated with this drug. Its high concentrations cause several serious effects including hepotoxicity and genotoxicity [5,6]. Unfortunately, it is evaluated as an emerging contaminant [6] and the development of sensitive and reliable

* Corresponding author at: Department of Pharmacy, Vocational School of Health Services, Bilecik Seyh Edebali University, 11100 Bilecik, Turkey.
E-mail address: gulsah.congur@bilecik.edu.tr (G. Congur).

https://doi.org/10.1016/j.microc.2024.112545
Received 18 July 2024; Received in revised form 5 November 2024; Accepted 19 December 2024
Available online 20 December 2024

analytical tools for PRL is essential.

Low detection limits were reported in various studies in the literature that were focused on spectroscopic and/or chromatographic monitoring of phenolic compounds [7–11]. However, their equipments are not suitable for the fabrication of miniaturized prototypes that can analyze the target molecules on-line. Electrochemical (bio)sensor technologies are one step closer to the miniaturization and to the development of commercial devices for field analyses in comparison to conventional techniques. Besides, they allow designing sustainable and feasible analytical tools with high sensitivity and selectivity [12–15].

Hydroxyapatite is the key component of bones and teeth. Its high durability, bioactivity and biocompatibility make it preferable in various biomedical applications from bone cement designs [16] to drug development [17]. Its nanoparticle form has a remarkable importance in the biosensor area for the development of cutting-edge designs towards the detection of nucleic acids [18,19], proteins [20–22], glucose [23,24], uric acid [25], etc. Hydroxyapatite nanoparticle (HaNP) based electrochemical sensor platforms were also reported in the literature for the monitoring of phenolic compounds [26–31]. Alam et al. [27] fabricated reduced graphene oxide/hydroxyapatite (rGO/HAp) nanocomposite, and modified glassy carbon electrode (GCE) surface with the nanocomposite using a nafion binder for the purpose of detection of bisphenol-A. They performed characterization studies of the nanocomposite structure using X-ray diffractometry (XRD), high-resolution transmission electron microscopy (HR-TEM), Fourier transform infrared spectroscopy (FT-IR), thermogravimetric analysis (TGA) and Raman spectroscopy. They evaluated the cytotoxicity of the nanocomposite by investigation of the proliferation behavior of human mesenchymal stem cells. They observed higher bisphenol-A signal using rGO/HAp/GCE in comparison to the one obtained by unmodified ones which was meant to sensitive and selective monitoring of bisphenol-A could be achieved using the developed electrode. They tested the applicability of the sensor in real life by analyzing different water samples. Although this sensor has various advantages, the main drawback of the design is the electrode type. GCE should be polished, and it requires doing extra pretreatment steps before use that make the said design less practical. The total fabrication time of the sensor is minimum 71 h and require applying heat at high temperatures, using extra chemical agents, and following exhaustive experimental steps. Similar drawbacks are for the study reported by Anitta and Sekar [28]. They developed a GCE-based electrochemical sensor for the monitoring of paracetamol and ciprofloxacin using hydroxyapatite sub-microparticles (C-HAP). Although they selected a natural source (cuttlefish bone) for the synthesis of C-HAP, the synthesis steps are long and require using extra agents and applying heat. Besides its drawbacks, C-HAP/GCE showed good analytical performance for the detection of paracetamol and ciproflaxin individually and simultaneously by using square wave technique (SWV).

To the best of our knowledge, there is no report in the literature for the development of HaNP modified single-use electrochemical sensor platform for the detection of PRL and PNL. Herein, a novel voltammetric sensor was designed taking the advantages of HaNP structure and using pencil graphite electrodes (PGEs). Enhanced surface area could be obtained after HaNP modification of PGE following a novel method. First, PGEs were chemically activated by NaOH, then, the modification of HaNPs prepared in an acidic media on the PGE surface was performed. Sensor parameters as NaOH concentration, activation time, HaNP concentration and modification time, pH, scan rate and concentration of PRL and PNL were meticulously evaluated. Selectivity of the sensor was investigated in the presence of inorganic and organic compounds, and real sample analysis was performed in drinking water and wastewater. Simultaneous detection of PRL and PNL was also evaluated. Finally, the greenness level of the sensor was investigated by performing green metric analysis. This is the first study in the literature for the fabrication of HaNP modified PGEs with the explained method, individual and simultaneous analyses of PRL/PNL using the developed sensor, and greenness evaluation of a PGE-based electrochemical sensor platform.

2. Materials and methods

2.1. Apparatus

The electrochemical measurements were performed using a potentiostat (IVIUM Compactstat.e with IVIUM Release 4.951 software package (Holland)) in a three-electrode system consisting of a working electrode (pencil graphite electrode (PGE)), a reference electrode (Ag/AgCl/3M KCl (BAS, Model RE-5B, W. Lafayette, USA) and a counter electrode (a platinum wire). For the preparation of the working electrode, the graphite lead (TOMBOW, HB) that is 6 cm of length was cut two equal parts, and each of them were used as a working electrode. Then, the graphite lead was placed into a pencil (Rotring, Germany) which was wrapped with a metallic wire through its body, and 10 mm of each lead was actively used during the activation/modification/measurement processes.

2.2. Chemicals

The hydroxyapatite nanoparticle (HaNP) solution (< 200 nm, stock concentration is 10^5 μg/mL), phenol (PNL), paracetamol (PRL) and the other chemicals such as and K_2HPO_4, KH_2PO_4, and NaCl, $K_3[Fe(CN)_6]$, $K_4[Fe(CN)_6]$, KCl, glucose, urea, $MgSO_4$, $CuSO_4$ and $ZnSO_4$ were supplied from Sigma-Aldrich (Germany). All chemicals were of analytical grade. Roundup and Hektafermine that are the commercial product of glyphosate and 2,4-dichlorophenoxyacetic acid, respectively were supplied from local market. Ibuprofen was donated by Assoc. Prof. Adem Şahin.

2.3. Procedure

2.3.1. HaNP/N-PGE fabrication

First, PGEs were chemically activated as in our previous studies using NaOH [32,33]. For the optimization of chemical activation conditions, NaOH concentration from 0.50 M to 2.00 M and activation time from 30 min to 120 min were studied. The PGEs activated by 1 M NaOH for 60 min were used for HaNP modification. Stock solution of HaNP was diluted in 1 % acetic acid solution prepared in ultrapure water to activate positively charged groups of HaNPs [34]. The activated PGEs (N-PGEs) were immersed into the 40 μL of 10–1500 μg/mL HaNP solution for 15 min at + 4°C for the modification. The effect of modification time was studied at 1000 μg/mL HaNP concentration level for 5–30 min. After the modification, the electrodes were washed with %1 acetic acid solution by immersing them into the solution for 5 s.

2.3.2. PRL/PNL analysis using N-PGEs or HaNP/N-PGEs

A three-electrode system was used for all electrochemical measurements. The N-PGEs or HaNP/N-PGEs placed into the pencil were directly immersed into the electrochemical cell contained 2 mL of PNL/PRL solution for the analysis.

For the investigation of the effects of pH and scan rate, 10 μg/mL PRL/PNL solution was used. The PNL/PRL solutions were prepared in 50 mM phosphate buffer solution containing 20.00 mM NaCl (PBS) at pH 3.00–5.00–7.00–11.00 for pH study, and PBS (pH 7.00) was used for scan rate study. The effect of PRL/PNL concentrations was studied at 5–30 μg/mL PRL and 10–30 μg/mL PNL concentration levels using CV technique. The effect of interference factors was investigated at 30 μg/mL concentration level. 0.00–5.00 μg/mL PRL/PNL were analyzed by DPV technique.

The real sample analysis and simultaneous detection of them were also performed by DPV technique. For real sample analysis, drinking water was boiled for less than 10 min and cooled at room temperature. Then, it was diluted by PBS (pH 7.00) using 1:1 dilution ratio. The wastewater obtained from the landfill leachate pool of a solid waste

management facility in Çanakkale province (40◦10′29″N26◦32′37″E) was used by 1:10 dilution with PBS (pH 7.00). PRL/PNL or their mixture were added into the water samples, and DPV measurements were conducted.

The stability of the N-PGEs and HaNP/N-PGEs were investigated by storing them at + 4°C for 28 days.

2.3.3. Voltammetric measurements

CV measurements were performed for the monitoring of activation/modification of PGEs based on the anodic peak current (I_a) of [K_4[Fe(CN)$_6$], and for PRL/PNL analysis. For the measurements of I_a value, 2.00 mM $K_3[Fe(CN)_6]/K_4[Fe(CN)_6]$ (1:1) contained in 0.10 M KCl was used as the redox probe. The measurements were done at a potential range from + 0.45 V to + 1.20 V with the scan rate as 50 mV/s. For the analysis of PRL/PNL, the measurements were performed at a potential range from −0.20 V to + 1.10 V with the scan rate as 50 mV/s. Scan rates ranging from 25 mV/s to 200 mV/s were applied to evaluate the effect of scan rate for PRL/PNL redox reaction process on the HaNP/N-PGE surface.

DPV measurements were done at a potential range from + 0.20 to + 0.80 V with the scan rate as 50 mV/s to monitor PRL/PNL at low concentrations and to analyze them in real samples.

2.3.4. AGREE analysis

The developed sensor system was evaluated in terms of its greenness level using Analytical GREEnness Metric Approach and Software (AGREE) [35]. In this approach, the 12 principles of green analytical chemistry (SIGNIFICANCE) are evaluated in 0–1 scale. This clock-like pictogram comprises of segments and red-yellow-green color scale that reflects each principle. The width of each segment depends on the weight of each principle, and the color of segments indicates the greenness level. Dark green represents the highest greenness while red indicates the lowest greenness.

3. Results and discussion

3.1. Development of HaNP/N-PGEs

In the first part of study, the results regarding the development of HaNP modified single-use electrochemical sensor platform were presented. First, the microscopic characterization of the HaNP modification was performed using SEM technique. The SEM images of PGEs, N-PGEs and HaNP/N-PGES are presented in Fig. 1. The graphite layers of the PGEs were clearly seen in Fig. 1A at each magnitude. The form of the layered surface changed after chemical activation as given in Fig. 1B, and the HaNP modification on the N-PGE surface was achieved as presented in Fig. 1C. The EDX results of C, O, Ca and P atoms supported the SEM images obtained each activation/modification step (Table S1, Fig. S1). The wt% and at% values of the O atom increased while the same values of Ca atom decreased after chemical activation which indicated the activation of –OH groups at the PGE surface was achieved. The wt% and at% values of the Ca and P atom sharply increased after HaNP modification of N-PGEs which was the expected result due to the introduction of Ca and P atoms of HaNP structure to the PGE surface.

The studies continued with the optimization of experimental conditions regarding the development of HaNP/N-PGEs. The effects of NaOH concentration and activation time were firstly investigated (Fig. S2 and S3). The changes % at the average I_a values obtained in the presence of 2.00 mM $K_3[Fe(CN)_6]/K_4[Fe(CN)_6]$ (1:1) contained in 0.10 M KCl were presented, and the I_a value decreased after NaOH activation which was the similar result given in the previous report [33]. The carboxyl groups could be activated after the chemical activation, and the PGE surface became negatively charged. There were repulsive interactions between carboxylated PGE surface and the negatively charged redox probe which caused the observation of a decrease trend at the average I_a value. The decrease ratio% increase while NaOH concentration increased. There were 26.03 % and 33.70 % decrease at the average I_a value (Fig. S2-c

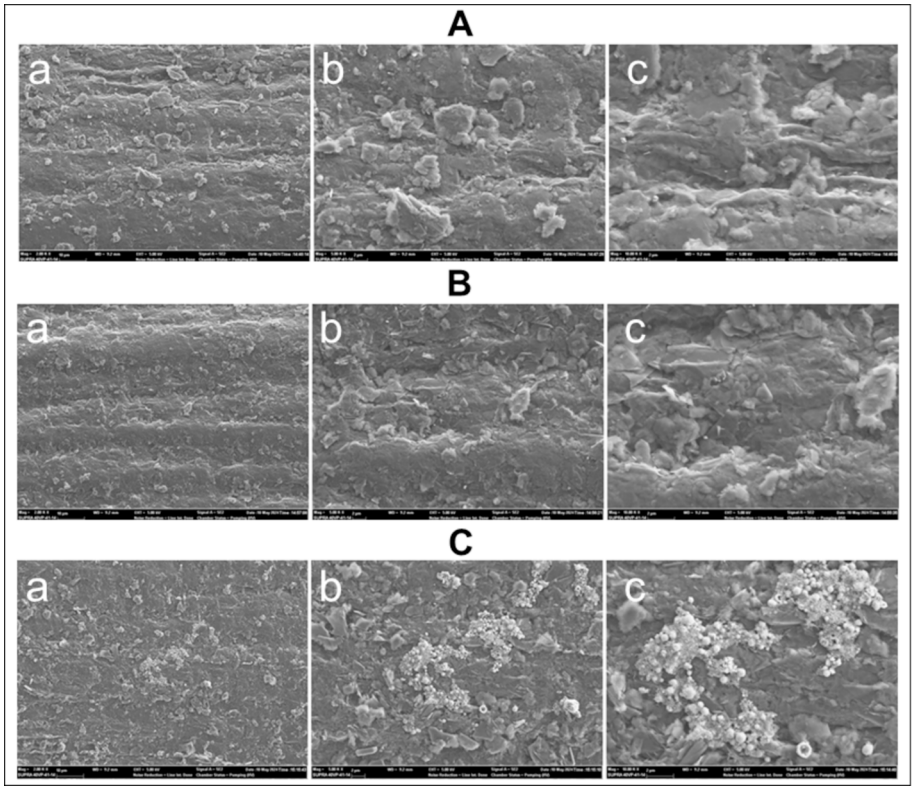

Fig. 1. SEM images of PGE **(A)**, N-PGE **(B)**, and HaNP/N-PGE **(C)**. The resolutions were selected as 2000x **(a)**, 5000x **(b)** and 10000x **(c)**, and the acceleration voltage was 5.0 kV. **The experimental conditions are: NaOH concentration:** 1 M, **NaOH activation time:** 1 h, **HaNP concentration:** 1000 μg/mL, **HaNP modification time:** 15 min. All measurements were done at Bilecik Seyh Edebali University Central Research Laboratory Application and Research Center.

and d, respectively) with the relative standard deviation % (RSD%) values 12.82 % and 18.35 % after the activation in the presence of 1.00 and 2.00 M NaOH, respectively. Since the reproducibility decreased while NaOH concentration increased, high concentration of NaOH did not studied, and the effect of the activation time was investigated using 1 and 2 M NaOH during 30–120 min (Fig. S3). The most reproducible average I_a value was obtained with 1 M NaOH activation during 60 min (Fig. S3-c) with the highest decrease% as 26.03% (RSD%= 12.82%, n = 3). 1.00 M NaOH concentration and 60 min activation time were selected as the optimum conditions for the chemical activation of the PGEs.

In the next step of the study, the effect of HaNP concentration upon the electrochemical sensor response was investigated (Fig. S4). For this purpose, N-PGEs were modified with 10–1500 μg/mL HaNP for 15 min. The average I_a value of N-PGEs was measured as 97.04 ± 8.52 μA (RSD %=8.78%, n = 3). The accumulation of positive charges on the HaNP structure occurred below pH 7.00 which its point of zero charge (PZC) value [34]. The PGE surface became positively charged after HaNP modification, and the repulsive interactions between electrode/electrolyte surface decreased that resulted in the increase at the average I_a value (Fig. S4A, a to b). The highest increase could be obtained in the presence of 1000 μg/mL HaNP. The average I_a value was found to be 120.18 ± 4.78 μA (RSD%= 3.98%, n = 3) using 1000 μg/mL HaNP/N-PGEs, and the increase ratio at the average I_a value was calculated as 23.84% (Fig. S4-B, a to e). The modification time was also optimized (Fig. S5) based on the increase at the average I_a values, and the highest increase (23.84%) and most reproducible result (RSD%= 3.98%, n = 3) could be obtained after 15 min modification (Fig. S5-A,B, a to c). The same increase was observed at the anodic charge value (Q_a). The average Q_a value of N-PGE was 6.22 ± 0.47 x10^{-4}C (RSD%= 7.63%, n = 3). After 1000 μg/mL HaNP modification for 15 min, this value increased and found to be 7.10 ± 0.40 x10^{-4}C (RSD%= 5.61%, n = 3). The behaviour of the Q_a value after HaNP modification on the N-PGE surface was in parallel with the behaviour of average I_a value. Therefore, 15 min modification time was chosen as optimum.

The effective surface area (A_{eff}) values of the PGE, N-PGE and 1000 μg/mL HaNP modified N-PGE were calculated using Randles and Sevcik Equation (Eq. 1) [36]. n, D and C values are the transferred electron number, the diffusion coefficient of $K_4[Fe(CN)_6]$ as 7.6 × 10^{-6} cm^2 /s, and the concentration of $K_4[Fe(CN)_6]$, respectively.

$$i_p = 2.6910^{-5} n^{3/2} A_{eff} D^{1/2} C v^{1/2}$$

The A_{eff} values of PGE, N-PGE and HaNP/N-PGE were found to be 0,345 cm^2, 0.262 cm^2 and 0.362 cm^2, respectively. These results indicated that HaNP modification provided enhanced effective surface area for the electrochemical analysis of PNL and PRL.

Repeatability of the developed HaNP/N-PGEs was studied (Figs. S6). Almost there were no differences at the average I_a values of the HaNP/N-PGEs in five different groups (n = 3). Stability of the HaNP-N/PGEs (Fig. S7-A) and N-PGEs (Fig. S7-B) was also investigated in this part of the study. HaNP-N/PGEs had stabile behavior during 28 day. However, there was instability at the response of N-PGEs (Fig. S7-B). These results indicate that stable and repeatable electrochemical sensor surface could be developed using HaNP-N/PGEs.

3.2. Voltammetric PRL detection using HaNP/N-PGEs

In the second part of the study, voltammetric PRL detection using HaNP-N/PGEs was studied. First, the effect of pH was investigated (Fig. S8). For this purpose, CV measurements were carried out in the presence of 10 μg/mL PRL at different pH values between 3.00 and 11.00. There were well-defined an oxidation (I_{PRLox}) and a reduction signal (I_{PRLred}) in the presence of 10 μg/mL PRL at each pH level. The peak potentials of I_{PRLox} and I_{PRLred} (E_{PRLox} and E_{PRLred}, respectively) shifted through more negative potential while pH value increased which was an evidence for the protonation of PRL molecules [37]. The slope of the pH versus E_{PRLox} graph was found to be −52.833 mV/pH that was close to 59 mV/pH defined as Nerstian theoretical value. This result indicated that proton transfer occurred during the quasi-reversible redox reaction of PRL [37]. The highest and the most reproducible I_{PRLox} could be measured at pH 7.00. This pH level was optimum for further studies.

The effect of scan rate upon the PRL redox reactions was then investigated (Fig. S9). There was a positive shift at the E_{PRLox} while a negative shift at the E_{PRLred} was observed from 25 mV/s to 200 mV/s (Fig. S9-A). Both I_{PRLox} and I_{PRLred} had linear behavior (Fig. S9-B) with the equations as y=0.02x+2.67 (R^2 = 0.9931) and y=-0.01x-2.73 (R^2 = 0.9875). The plots of the log current vs log scan rate (Fig. S10-A) and current vs square root of scan rate (Fig. S10-B) were also investigated. Both plots had linear behaviors in terms of both I_{PRLox} and I_{PRLred} values. When the slopes of the equations obtained from log current vs log scan rate graphs equal to 1, the redox process is surface-controlled. Due to the fact that square root of scan rate plots were linear for both I_{PRLox} and I_{PRLred} values with the R^2 = 0.9938 and 0.9767, respectively, and the slopes of the log current vs log scan rate were not equal to 1, it can be concluded that the redox reaction of PRL at HaNP/N-PGE surface was a typical diffusion-controlled process [38–40].

The HaNP/N-PGEs were used for the investigation of the PRL detection at different concentration levels using CV technique (Fig. S11). 5–30 μg/mL PRL samples were analyzed using HaNP/N-PGEs and the I_{PRLox} measured at + 0.440 V increased while the concentration level of PRL increased. The limit of detection (LOD) was calculated with the equation as y = 0.48x-0.47 (R^2 = 0.9963) [41] and found to be 1.72 μg/mL (11.37 μM). The same analysis was conducted using N-PGEs and the LOD was found to be 2.22 μg/mL (14.69 μM) with the equation as y = 0.48x-0.45 (R^2 = 0.9938) (Fig. S12). These results showed that lower LOD value of PRL could be obtained using HaNP/N-PGEs compared to the one obtained by N-PGEs.

The selectivity of the developed electrochemical sensor in terms of PRL detection was tested in the presence of 30 μg/mL PRL and 30 μg/mL interference factors (Figs. S13 and S14). The compounds used in the selectivity study were chosen as they are ions that could be found in the water and emerging contaminants that could be detected in water sources and wastewaters [42–45]. There were negligible control signals of the selected interference factors and they were given in Fig. S13. The change ratios% at the I_{PRLox} obtained in the present of different inorganic and organic compounds were calculated (Fig. S14). In the presence of KCl, $MgSO_4$, $CuSO_4$, urea, roundup, hektafermine, ibuprofen and glucose, the average sensor response was changed as 0.60 %, 9.86 %, 5.16 %, 11.84 %, 2.72 %, 2.59 %, 11.30 %, 13.15 %, and 0.21 %, respectively. The interferences did not affect the sensor response remarkably, and it was concluded that the HaNP/N-PGE based electrochemical sensor platform could selectively detect PRL even in the presence of different interference factors.

In the next step of this part of the study, voltammetric PRL analysis was performed using DPV technique which is more sensitive technique compared to CV technique (Fig. 2). 0.25–4.00 μg/mL PRL was analyzed by using HaNP/N-PGEs, and a linear calibration graph based on the I_{PRLox} signal measured at + 0.375 V could be obtained in the concentration range from 1.00 to 4.00 μg/mL with the equation as y = 537.38x-41.41 (R^2 = 0.9963). The LOD value was found to be 0.19 μg/mL (1.26 μM) [41]. The same experiment was done in the presence of 1.00–4.00 μg/mL PRL prepared in drinking water:PBS (pH 7.00) (1:1) and wastewater: PBS (pH 7.00) (1:10) (Fig. S15 and S16, respectively). The LOD values were found to be 0.06 μg/mL (0.39 μM) and 0.09 μg/mL (0.59 μM) [41] for drinking water and wastewater analysis, respectively.

3.3. Voltammetric PNL detection using HaNP/N-PGEs

In the third part of the study, the electrochemical detection of PNL using HaNP/N-PGEs was investigated. Similar to the second part, the

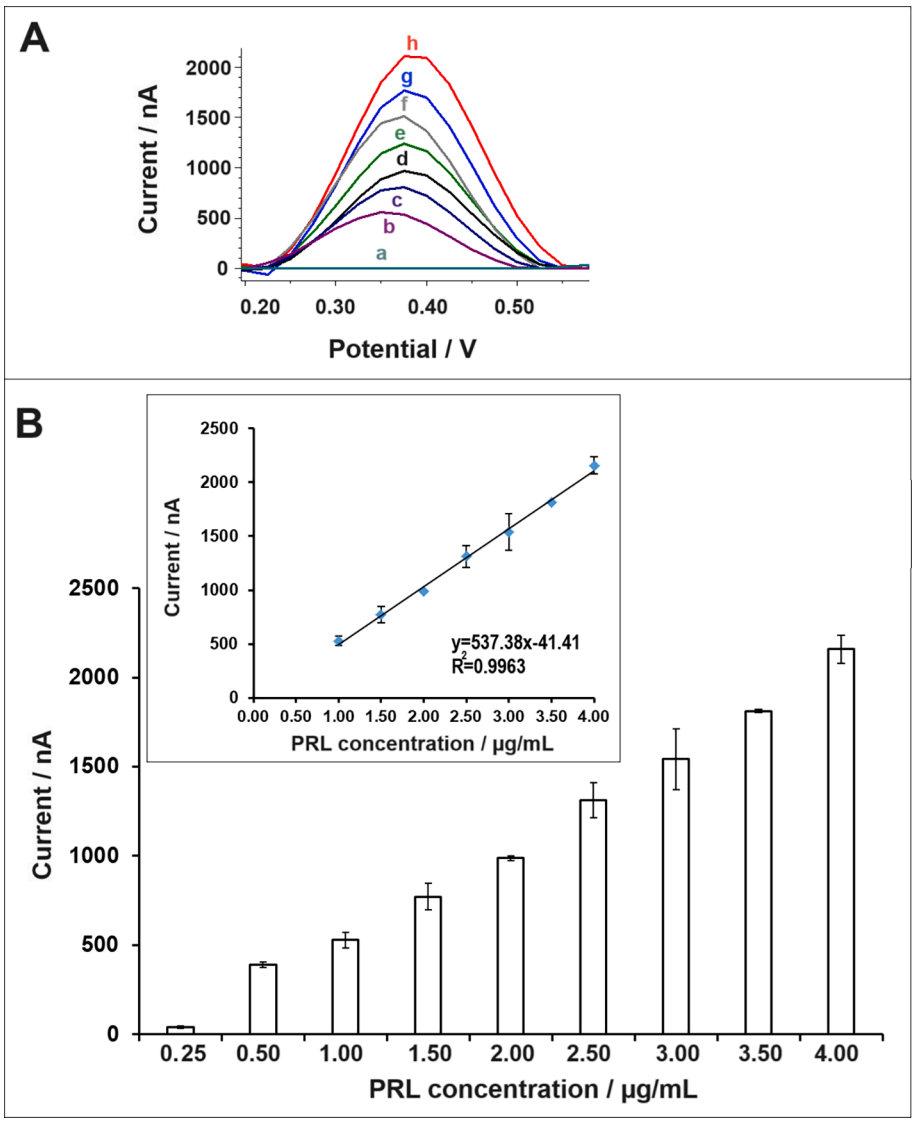

Fig. 2. The voltammograms **(A)** representing the control signal of HaNP/N-PGE in PBS (pH 7.00) **(a)**, the oxidation signals of 1.00 **(b)**, 1.50 **(c)**, 2.00 **(d)**, 2.50 **(e)**, 3.00 **(f)**, 3.50 **(g)** and 4.00 **(h)** µg/mL PRL in PBS (pH 7.00). Histograms **(B)** representing the I_{PRLox} values of 0.25–4.00 µg/mL PRL (n = 3). **Inset:** The linear calibration graph represented the average I_{PRLox} values of 1.00–4.00 µg/mL PRL (n = 3). All measurements were done by DPV technique. **Scan rate:** 50 mV/s.

effect of pH upon the sensor response was studied firstly. As seen in Fig. S17, E_{PNLox} was negatively shifted while pH increased from 3 to 11, and a linear pH versus E_{PNLox} graph could be obtained with the equation as y=-0.05x+1.04 ($R^2 = 0.9921$). The highest PNL signal was monitored at pH 7.00, and this pH value was selected as optimum for PNL detection. Then, the effect of scan rate was investigated to evaluate PNL oxidation process occurred at the HaNP/N-PGE surface (Fig. S18). Although there were one I_{PNLox} and two I_{PNLred} measured at around + 0.680 V, −0.010 V and + 0.260 V, respectively, the I_{PNLox} and the I_{PNLred} measured at −0.010 V were evaluated due to the fact that the other reduction signal seemed to be an overlapped signal of two different signals. The signals linearly increased while scan rate increased. Linear graphs could be obtained for I_{PNLox} and I_{PNLred} signals with the equations as y = 0.054 + 5.35 ($R^2 = 0.9843$), y = -0.005–0.09 ($R^2 = 0.9817$) (Fig. S18-B). Moreover, the behaviors of I_{PRLox} and I_{PRLred} signals were linear in the square root of scan rate plot (Fig. S19-B-II) with the R^2 = 0.9991 and 0.9936, respectively, and the slope of the plots of the log current vs log scan rate were smaller than 1 (Fig. S219-B-I). Therefore, it can be concluded that the redox reaction of PNL at HaNP/N-PGE surface was a diffusion-controlled process [38–40].

The electrochemical detection of PNL using both HaNP/N-PGEs (Fig. S20) and N-PGEs (Fig. S21) was performed using CV technique. 10–30 µg/mL PNL was analyzed, and there was a linear increase at the I_{PNLox} while the concentration increased. The LOD values were calculated [41] and found to be 0.64 µg/mL (6.80 µM) and 1.78 µg/mL (18.91 µM) with the equations as y = 0.65x + 2.46 ($R^2 = 0.9993$) and y = 0.76x-0.08 ($R^2 = 0.9944$) using HaNP/N-PGEs and N-PGEs, respectively. Lower LOD value of PNL could be obtained using HaNP/N-PGEs with better R^2 value compared to the one obtained using N-PGEs. The selectivity of the sensor was studied in terms of PNL analysis using CV technique (Fig. S22). 30 µg/mL PNL was analyzed in the presence of 30 µg/mL interference factors. In the presence of KCl, $MgSO_4$, $CuSO_4$, urea, roundup, hektafermine, ibuprofen and glucose, the average sensor response was changed as 7.10 %, 17.13 %, 3.33 %, 9.60 %, 10.10 %, 17.43 %, 9.44 %, 7.73 %, and 3.25 %, respectively. Although changes at the sensor response were observed in the presence of different analytes, the HaNP/N-PGE based voltammetric sensor could still detect PNL selectively.

The voltammetric PNL analysis was also studied using DPV technique at 0.50–4.00 µg/mL concentration level (Fig. 3). The I_{PNLox} measured at + 0.650 V increased till the concentration increased, and a linear calibration graph could be obtained at this concentration range

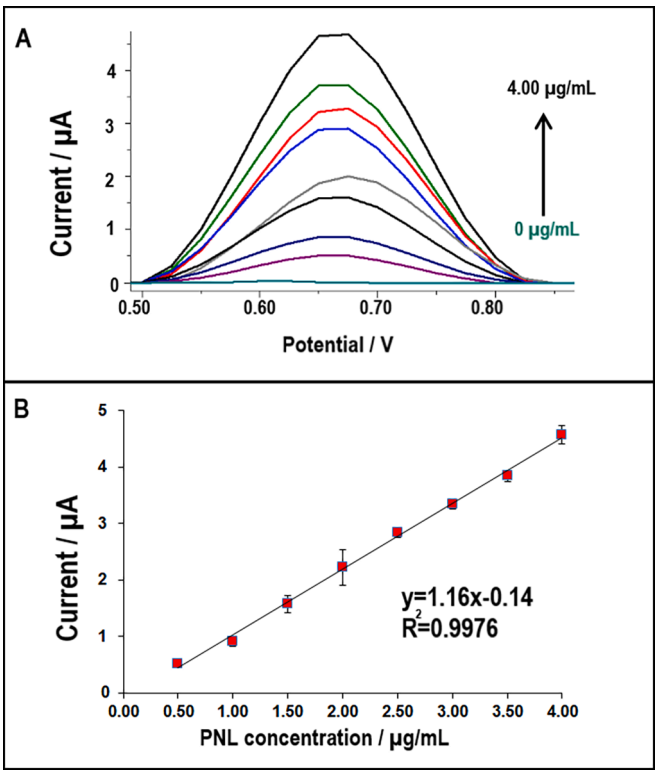

Fig. 3. The voltammograms **(A)** representing the oxidation signals of 0.00–4.00 µg/mL PNL measured by DPV technique. The line graph **(B)** representing the average oxidation signals of 0.50–4.00 µg/mL PRL (n = 3). **Scan rate:** 50 mV/s.

with the equation as y = 1.16x-0.14 (R^2 = 0.9976). The LOD was found to be 0.18 µg/mL (1.91 µM) [41]. Figs. S23 and S24 represent the voltammetric analysis of PNL in drinking water:PBS (pH 7.00) (1:1) and in wastewater:PBS (pH 7.00) samples. The LOD values were also calculated [41] and found to be 0.08 µg/mL (0.85 µM) and 0.17 µg/mL (1.80 µM) with the equations as y = 405.20x + 38.80 (R^2 = 0.9984) and y = 1.01x + 0.14 (R^2 = 0.9970) in drinking water and wastewater samples, respectively.

3.4. Simultaneous detection of PRL and PNL using HaNP/N-PGEs

In this part, PRL and PNL were analyzed simultaneously using DPV technique in order to investigate whether HaNP/N-PGE-based electrochemical sensor could detect of PRL and PNL (Fig. 4). Well-defined two peaks of PRL and PNL could be observed at + 0.375 V (Fig. 4-I) and + 0.650 V (Fig. 4-II), respectively. While one of the analyte concentrations was kept constant at 2.00 µg/mL concentration level, the concentration of the other one was increased from 1.00 to 5.00 µg/mL. A linear increase at PRL (Fig. 4-I) and PNL (Fig. 4-II) signals, and the calibration graphs could be obtained (Fig. 4-III and IV). LOD, LOQ and sensitivity values were calculated [41] (Table S2), and these values were close to the ones obtained in PBS (pH 7.00) while individual detection of the analytes was performed. The detection of the analytes was tested in wastewater (Fig. S25). Linear increase at the PRL and PNL signals could be observed (Fig. S25-A) and LOD, LOQ and sensitivity values were calculated (Table S2) based on the linear graphs given in Fig. S25-B and C [41]. These results indicated that HaNP/N-PGE-based voltammetric sensor could simultaneously detect PRL and PNL.

The LOD values, limit of quantification (LOQ) and sensitivity values of PRL and PNL were given in Table S2. Tables S3 and S4 represent previous studies for the electrochemical detection of PRL [37,46–54] and PNL [55–63], respectively. The LOD values obtained in this study are comparable with the reported LOD values in previous studies. On the other hand, the HaNP/N-PGEs could be developed in just 1 h 15 min which is quite lower fabrication time in comparison to the reported studies. The nanomaterials or their composite structures have been widely applied for the improvement of sensor parameters such as sensitivity, selectivity and stability as given in Tables S3 and S4. However, these applications should be carried out without using excessive chemicals or any further physical or chemical treatments as much as possible. Although most of the sensor given in the tables could reach low detection limits, their fabrication processes were exhaustive and controversial in terms of greenness. As an example, Shih and coworkers synthesized zeolitic imidazolate frameworks and graphene oxide (ZIF-GO) derived ^{3}D–^{2}D Zn/N-doped carbon (ZnNC-rGO) nanocomposite, and modified at the surface of GCE for the purpose of voltammetric PRL detection [48]. They reached a low LOD as 0.077 µM using ZnNC-rGO/GCE. However, total fabrication time of the sensor was approximately 16 h that required applying heat at high temperature as 500–900 °C. In another study, Meng et al. [61] developed Fe_2O_3/MIL-53(Fe)/rGO metal–organic framework (MOF) modified GCE for the voltammetric detection of PNL. They found the LOD value as 0.10 µM using Fe_2O_3/MIL-53(Fe)/rGO/GCE and linear sweep voltammetry (LSV) technique. Although the LOD was quite lower than other LOD values given in the Table S4, the fabrication time of the sensor was long and required applying exhaustive and non-environmentally friendly experimental steps such as applying heat at high temperature as 400 °C, and using organic chemicals.

When it comes to the evaluation of the electrochemical sensors in terms of development of easy-to-use designs, the type of working electrode is extremely important. At this point, single-use electrodes such as PGEs and screen printed electrodes (SPE) are one step further than the other electrodes such as carbon paste electrodes (CPE) and GCE that require non-practical pretreatment steps such as filling, sonication and polishing. Moreover, these extra steps require using extra chemical agents which make the sensor platform less green and labor-friendly. Most of the studies represented in the Tables S3 and S4 were based on the use of GCEs and CPEs which makes them more disadvantageous than the present study. The development procedure of the HaNP/N-PGEs was quite practical and did not require to use any extra chemical agents or to apply heat. Furthermore, HaNP/N-PGE-based electrochemical sensor has a great potential for field applications since different water samples could be analyzed in terms of PRL/PNL detection using HaNP-N/PGEs.

3.5. AGREE analysis of the voltammetric sensor developed based on the HaNP/N-PGEs

The AGREE analysis results of each SIGNIFICANCE criteria produced by AGREE software were given in Table S5, and the pictogram generated by the software was given in Fig. 5. The scores of Criteria 3 and 10 were 0 since the analysis of PRL and PNL were performed in the laboratory and the chemicals are not renewable. Although HaNP can be produced by natural sources, it was purchased and its source was not known. Therefore, Criteria 10 was determined as 0. Another low score was for Criteria 1 due to the fact that real sample analysis requires extra pretreatment steps as dilution and heating for a short time which brought extra steps to the development procedure. Other criteria were quite close to 1 which made the sensor platform close to the highest greenness. As explained from Pena-Pereira et al. [35], miniaturization allows fabricating green systems since sample requirement can be reduced. Metal electrodes such as platinum electrode and gold electrode, and carbon electrodes such as GCE and CPE are disadvantageous in terms of SIGNIFICANCE due to the fact that their preparation requires applying extra pretreatment steps as explained before. It should be pointed out that PGEs-based electrochemical sensor platforms are the prototypes for more miniaturized systems and require using low sample volume of chemicals. Another important point highlighted by Pena-Pereira et al. [35] is to minimize energy and extra chemical agents consuming during

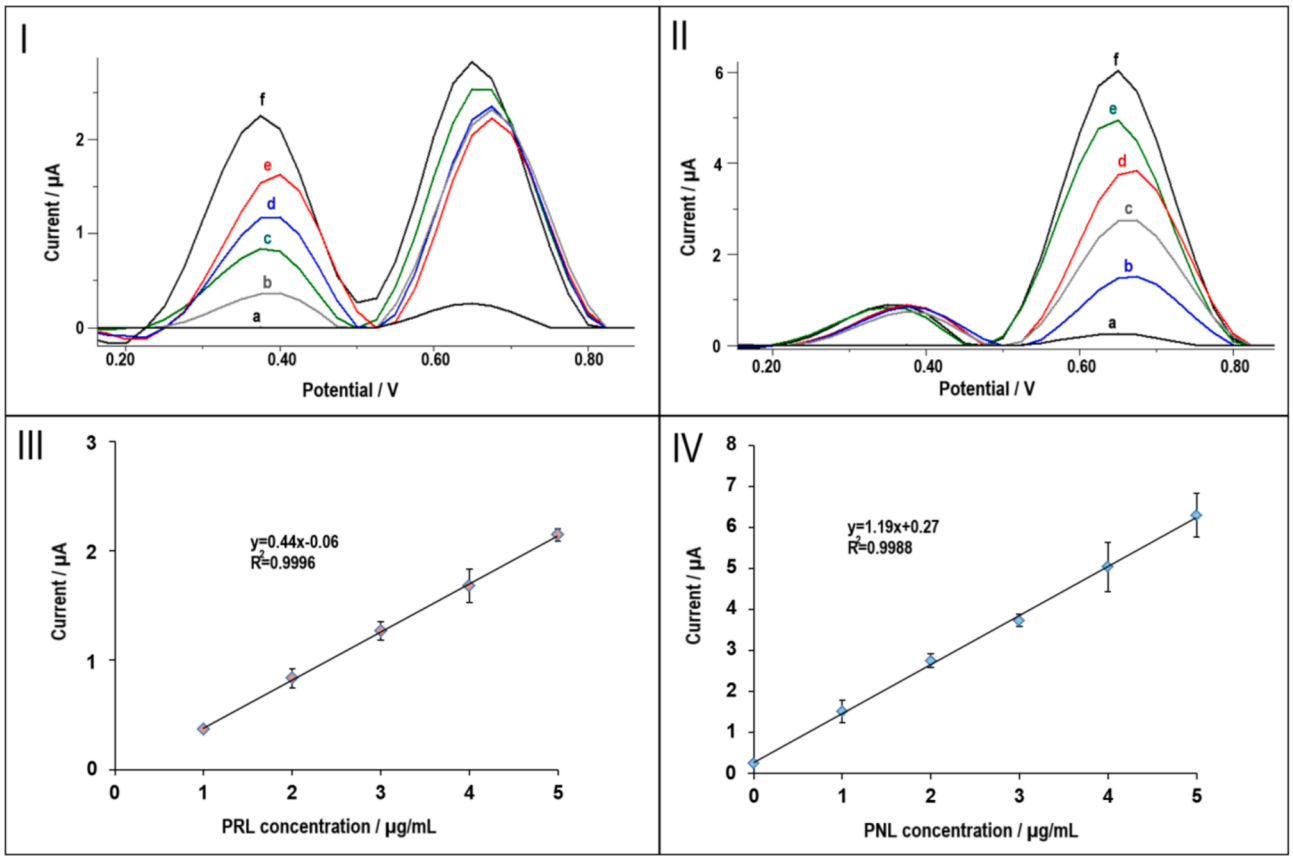

Fig. 4. Voltammograms of I_{PRLox} **(I)** and I_{PNLox} **(II)** obtained in the presence of 2.00 µg/mL PNL: 1.00–5.00 µg/mL PRL (1:1), or 2.00 µg/mL PRL: 1.00–5.00 µg/mL PNL (1:1). Control signal of HaNP/N-PGE **(a)**, 1.00 **(b)**, 2.00 **(c),** 3.00 **(d),** 4.00 **(e),** and 5.00 **(f)** µg/mL PRL or PNL. Line graphs representing the average I_{PRLox} **(III)** and I_{PNLox} **(IV)** values obtained in the presence of 2.00 µg/mL PNL: 1.00–5.00 µg/mL PRL (1:1), or 2 µg/mL PRL: 1.00–5.00 µg/mL PNL (1:1). **Scan rate:** 50 mV/s.

Fig. 5. The pictogram of AGREE analysis results of the HaNP/N-PGEs based voltammetric electrochemical sensor.

the development process. Most of the chromatographic and spectroscopic techniques are evaluated as less green or non-green in AGREE analysis whereas electrochemical analytical techniques are evaluated one of the closer group to the greenness. Therefore, the HaNP/N-PGEs have numerous superior properties in terms of greenness in comparison to not only chromatographic or spectroscopic techniques but also the sensor platforms given in Table S3 and S4 which required heat application at high temperatures for fabrication [46,48–59,61–63].

4. Conclusion

In this study, two major contaminants found in water, PRL and PNL were analyzed by using a novel electrochemical sensor platform. Single-use PGEs were chemically activated, and modified with HaNPs. The HaNP/N-PGEs showed repeatable, stable and selective behavior. Simultaneous voltammetric detection of PRL and PNL was also performed using HaNP/N-PGEs. Low LOD values of PRL and PNL were reached using DPV technique for not only buffer solution but also drinking water and wastewater samples, and simultaneous detection. High greenness level of the developed voltammetric sensor platform was obtained by AGREE software. This study has novelty in terms of (i) development of HaNP/N-PGEs, (ii) voltammetric PRL and PNL detection using HaNP/N-PGEs, (iii) simultaneous detection of PRL and PNL using the HaNP/N-PGEs, and (iv) greenness evaluation of a PGE-based electrochemical sensor platform using AGREE software. The developed electrochemical sensor platform has a great capacity for designing future green hand-held devices that will be able to perform on-line analysis of the selected analytes.

CRediT authorship contribution statement

Gulsah Congur: Writing – review & editing, Writing – original draft, Visualization, Validation, Supervision, Resources, Project administration, Methodology, Investigation, Funding acquisition, Formal analysis, Conceptualization. **Elif Efe:** Investigation, Formal analysis.

Declaration of competing interest

The authors declare that they have no known competing financial

interests or personal relationships that could have appeared to influence the work reported in this paper.

Acknowledgements

GC, as the team captain of the Hi-SENS team (team ID: 291555), would like to thank Bilecik Şeyh Edebali University Rectorate for supporting this work as a TEKNOFEST project within the scope of TEKNOFEST'24 organization. GC also would like to present her appreciation to The Turkish Technology Team within the scope of TEKNOFEST'24 organization for the evaluation and presentation process of the project in Environment and Energy Technologies category. The project ID is 2005818 and the project title is "Hydroxyapatite Nanoparticles Modified Disposable Electrochemical Chip Technology for the Detection of Water Pollutants Paracetamol and Phenol". GC would also like to thank Assoc. Prof. Adem Şahin for the donation of ibuprofen, and Erdem Nazilli for supplying wastewater samples.

Appendix A. Supplementary data

Supplementary data to this article can be found online at https://doi.org/10.1016/j.microc.2024.112545.

Data availability

The data that has been used is confidential.

References

[1] W. Strugała-Wilczek, K. Basa, K. Kapusta, Soukup, In situ sorption phenomena can mitigate potential negative environmental effects of underground coal gasification (UCG) - an experimental study of phenol removal on UCG-derived residues in the aspect of contaminant retardation, Ecotoxicol. Environ. Saf. 208 (2021) 111710, https://doi.org/10.1016/j.ecoenv.2020.111710.

[2] Z. Ghahghaey, M. Hekmati, M.D. Ganji, Theoretical investigation of phenol adsorption on functionalized graphene using DFT calculations for effective removal of organic contaminants from wastewater, J. Mol. Liq. 324 (2021) 114777, https://doi.org/10.1016/j.molliq.2020.114777.

[3] D.T. Nguyen, H.N. Tran, R.-S. Juang, N.D. Dat, F. Tomul, A. Ivanets, S.H. Woo, A. Hosseini-Bandegharaei, H.-P. Chao, Adsorption process and mechanism of acetaminophen onto commercial activated carbon, J. Environ. Chem. Eng. 8 (2020) 104408, https://doi.org/10.1016/j.jece.2020.104408.

[4] H.N. Tran, F. Tomul, N.T.H. Ha, D.T. Nguyen, E.C. Lima, G.T. Le, C.-T. Chang, V. Masindi, S.H. Woo, Innovative spherical biochar for pharmaceutical removal from water: Insight into adsorption mechanism, J. Hazard. Mater. 394 (2020) 122255, https://doi.org/10.1016/j.jhazmat.2020.122255.

[5] C.M. Kerkhoff, K. da Boit Martinello, D.S. Franco, M.S. Netto, J. Georgin, E. L. Foletto, D.G. Piccilli, L.F. Silva, G.L. Dotto, Adsorption of ketoprofen and paracetamol and treatment of a synthetic mixture by novel porous carbon derived from *Butia capitata* endocarp, J. Mol. Liq. 339 (2021) 117184, https://doi.org/10.1016/j.molliq.2021.117184.

[6] A. Islam, M.K. Nazal, A.A. Akinpelu, M. Sajid, N.A. Alhussain, M. Ilyas, High performance adsorptive removal of emerging contaminant paracetamol using a sustainable biobased mesoporous activated carbon prepared from palm leaves waste, J. Anal. App. Pyrol. 180 (2024) 106546, https://doi.org/10.1016/j.jaap.2024.106546.

[7] W. Zhu, R. Yang, N. Zhao, G. Yin, J. Liu, Determination of phenolic compounds in water using a multivariate statistical analysis method combined with three-dimensional fluorescence spectroscopy, RSC Adv. 14 (2024) 2235–2242, https://doi.org/10.1039/d3ra06917f.

[8] X. Li, Y.Y. Cui, C.X. Yang, X.P. Yan, Synthesis of carboxyl functionalized microporous organic network for solid phase extraction coupled with high-performance liquid chromatography for the determination of phenols in water samples, Talanta 208 (2020) 120434, https://doi.org/10.1016/j.talanta.2019.120434.

[9] D.G. Carvalho, L. Ranzan, R.A. Jacques, L.F. Trierweiler, J.O. Trierweiler, Analysis of total phenolic compounds and caffeine in teas using variable selection approach with two-dimensional fluorescence and infrared spectroscopy, Microchem. J. 169 (2021) 106570, https://doi.org/10.1016/j.microc.2021.106570.

[10] N. Amareh, Y. Yamini, M. Saeidi, Z. Dinmohammadpour, M. Nazraz, Synthesis, characterization and application of ZIF-7@ZIF-67/PES for dispersive solid phase extraction of bisphenol A and 2-phenyl phenol, Talanta Open 8 (2023) 100269, https://doi.org/10.1016/j.talo.2023.100269.

[11] R. Sun, Y. Wang, Y. Ni, S. Kokot, Spectrophotometric analysis of phenols, which involves a hemin–graphene hybrid nanoparticles with peroxidase-like activity, J. Hazard. Mater. 266 (2014) 60–67, https://doi.org/10.1016/j.jhazmat.2013.12.006.

[12] H. Kumar, N. Kumari, R. Sharma, Nanocomposites (conducting polymer and nanoparticles) based electrochemical biosensor for the detection of environment pollutant: Its issues and challenges, Environ. Impact Assess. Rev. 85 (2020) 106438, https://doi.org/10.1016/j.eiar.2020.106438.

[13] X. Gu, B. Su, C. Liu, S. Zheng, Y. Wang, J. Tian, L. Ma, Wu, Recent progress in advanced materials for electrochemical determination of phenolic contaminants, Microchem. J. 195 (2023) 109513, https://doi.org/10.1016/j.microc.2023.109513.

[14] J. Mohanapriya, S. Satija, V.K. Senthilkumar, K. Ponnusamy, Thenmozh, Design and engineering of 2D MXenes for point-of-care electrochemical detection of bioactive analytes and environmental pollutants, Coord. Chem. Rev. 507 (2024) 215746, https://doi.org/10.1016/j.ccr.2024.215746.

[15] M. Liang, Y. Liu, S. Lu, Y. Wang, C. Gao, K. Fan, H. Li, Two-dimensional conductive MOFs toward electrochemical sensors for environmental pollutants, TrAC Trend. Anal. Chem. 177 (2024) 117800, https://doi.org/10.1016/j.trac.2024.117800.

[16] R. Karpiński, J. Szabelski, P. Krakowski, J. Jonak, K. Falkowicz, M. Jojczuk, A. Nogalski, A. Przekora, Effect of various admixtures on selected mechanical properties of medium viscosity bone cements: Part 2 – Hydroxyapatite, Compos. Struct. 343 (2024) 118308, https://doi.org/10.1016/j.compstruct.2024.118308.

[17] M.S. Asghar, U. Ghazanfar, M. Idrees, M.S. Irshad, Z. Haq, M.Q. Javed, S.Z. Hassan, M. Rizwan, In vitro controlled drug delivery of cationic substituted hydroxyapatite nanoparticles; enhanced anti-chelating and antibacterial response, Kuwait J. Sci. 50 (2023) 97–104, https://doi.org/10.1016/j.kjs.2023.02.014.

[18] G. Congur, A. Erdem, Impedimetric monitoring of microRNA-200c-3p using hydroxyapatite nanoparticles modified pencil graphite electrodes, J. Mater. Sci. (2024), https://doi.org/10.1007/s10853-024-09832-w.

[19] K.S. Rizi, B. Hatamluyi, M. Rezayi, Z. Meshkat, M. Sankian, K. Ghazvini, H. Farsiani, E. Aryan, Response surface methodology optimized electrochemical DNA biosensor based on HAPNPTs/PPY/MWCNTs nanocomposite for detecting *Mycobacterium tuberculosis*, Talanta 226 (2021) 122099, https://doi.org/10.1016/j.talanta.2021.122099.

[20] Y. Zhang, Y. Xia, F. Zhang, Z. Wang, Q. Liu, Ultrasensitive label-free homogeneous electrochemical aptasensor based on sandwich structure for thrombin detection, Sens. Act. B. Chem. 267 (2018) 412–418, https://doi.org/10.1016/j.snb.2018.04.053.

[21] F. Qu, M. Yang, A. Rasooly, Dual signal amplification electrochemical biosensor for monitoring the activity and inhibition of the Alzheimer's related protease β-secretase, Anal. Chem. 88 (2016) 10559–10565, https://doi.org/10.1021/acs.analchem.6b02659.

[22] Y. Huang, C. Tang, J. Liu, J. Cheng, Z. Si, T. Li, M. Yang, Signal amplification strategy for electrochemical immunosensing based on a molybdophosphate induced enhanced redox current on the surface of hydroxyapatite nanoparticles, Microchim. Acta. 184 (2017) 855–861, https://doi.org/10.1007/s00604-016-2069-z.

[23] J. Li, D. Kuang, Y. Feng, F. Zhang, M. Liu, Glucose biosensor based on glucose oxidase immobilized on a nanofilm composed of mesoporous hydroxyapatite, titanium dioxide, and modified with multi-walled carbon nanotubes, Microchim. Acta 176 (2012) 73–80, https://doi.org/10.1007/s00604-011-0693-1.

[24] G. Bharath, R. Madhu, S.M. Chen, V. Veeramani, A. Balamurugan, D. Mangalaraj, C. Viswanathan, N., Ponpandian enzymatic electrochemical glucose biosensors by mesoporous 1D hydroxyapatite-on-2D reduced graphene oxide, J. Mater. Chem. B. 3 (2015) 1360–1370. https://pubs.rsc.org/en/content/articlehtml/2015/tb/c4tb01651c.

[25] Y. Chen, W. Zhou, J. Ma, F. Ruan, X. Qi, Y. Cai, Potential of a sensitive uric acid biosensor fabricated using hydroxyapatite nanowire/reduced graphene oxide/gold nanoparticle, Microsc. Res. Tech. 83 (2020) 268–275, https://doi.org/10.1002/jemt.23410.

[26] N. Lavanya, N. Sudhan, P. Kanchana, S. Radhakrishnan, C. Sekar, A new strategy for simultaneous determination of 4-aminophenol, uric acid and nitrite based on graphene/hydroxyapatite composite modified glassy carbon electrode, RSC Adv. 5 (2015) 52703–52709, https://doi.org/10.1039/C5RA06763D.

[27] M.K. Alam, M.M. Rahman, A. Elzwawya, S.R. Torati, M.S. Islam, M. Todo, A. M. Asiri, D. Kim, C.G. Kim, Highly sensitive and selective detection of Bisphenol A based on hydroxyapatite decorated reduced graphene oxide nanocomposites, Electrochim. Acta 241 (2017) 353–361, https://doi.org/10.1016/j.electacta.2017.04.135.

[28] S. Anitta, C. Sekar, Voltammetric determination of paracetamol and ciprofloxacin in the presence of vitamin C using cuttlefish bone-derived hydroxyapatite sub-microparticles as electrode material, Result. Chem. 5 (2023) 100816, https://doi.org/10.1016/j.rechem.2023.100816.

[29] L. Lu, L. Zhang, X. Zhang, S. Huan, G. Shen, R. Yu, A novel tyrosinase biosensor based on hydroxyapatite–chitosan nanocomposite for the detection of phenolic compounds, Anal. Chim. Acta 665 (2010) 146–151, https://doi.org/10.1016/j.aca.2010.03.033.

[30] N. Sudhan, C. Manikkaraj, V. Balasubramanian, G. Archunan, C. Sekar, Electrochemical detection of estrus specific phenolic compound p-cresol to assess the reproductive phase of certain farm animals, Biochem. Eng. J. 126 (2017) 78–85, https://doi.org/10.1016/j.bej.2017.06.012.

[31] H. Yin, Y. Zhou, S. Ai, X. Liu, L. Zhu, L. Lu, Electrochemical oxidative determination of 4-nitrophenol based on a glassy carbon electrode modified with a hydroxyapatite nanopowder, Microchim. Acta 169 (2010) 87–92, https://doi.org/10.1007/s00604-010-0309-1.

[32] G. Congur, Development of a novel methyl germanane modified disposable sensor and its application for voltammetric phenol detection, Surf. Inter. 25 (2021) 101268, https://doi.org/10.1016/j.surfin.2021.101268.

[33] G. Congur, Ü.D. Gül, Phenol monitoring in water samples using an inexpensive electrochemical sensor based on pencil electrodes modified with DTAB surfactant, J. Env. Chem. Eng. 9 (2021) 105804, https://doi.org/10.1016/j.jece.2021.105804.
[34] I.S. Harding, N. Rashid, K.A. Hing, Surface charge and the effect of excess calcium ions on the hydroxyapatite surface, Biomaterial. 26 (2005) 6818–6826, https://doi.org/10.1016/j.biomaterials.2005.04.060.
[35] F. Pena-Pereira, W. Wojnowski, M. Tobiszewski, AGREE:Analytical GREEnness Metric Approach and Software, Anal. Chem. 92 (2020) 10076–10082, https://doi.org/10.1021/acs.analchem.0c01887.
[36] T.E. Cummings, P.J. Elving, Determination of the electrochemically effective electrode area, Anal. Chem. 50 (1978) 480–488, https://doi.org/10.1021/ac50025a031.
[37] L. Magerusan, F. Pogacean, S. Pruneanu, Enhanced acetaminophen electrochemical sensing based on nitrogen-doped graphene, Int. J. Mol. Sci. 23 (2022) 14866, https://doi.org/10.3390/ijms232314866.
[38] A. Pollap, K. Baran, N. Kuszewska, J. Kochana, Electrochemical sensing of ciprofloxacin and paracetamol in environmental water using titanium sol based sensor, J. Electroanal. Chem. (2020) 878 114574. 10.1016/j.jelechem.2020.114574.
[39] Z. Masood, H. Muhammad, I.A. Tahiri, Comparison of different electrochemical methodologies for electrode reactions: A case study of paracetamol, Electrochem. 5 (2024) 57–69, https://doi.org/10.3390/electrochem5010004.
[40] O. Yolchuyev, Z. Aydogmus, Electrochemical behavior and differential pulse voltammetric determination of budesonide in suspension ampoules, Istanbul J. Pharm. 53 (2023) 150–158, https://doi.org/10.26650/IstanbulJPharm.2023.1093821.
[41] J.N. Miller, J.C. Miller. Statistics and Chemometrics for Analytical Chemistry, sixth ed., Pearson Education, Essex (2005) pp. 121–12.
[42] S. Chopra, D. Kumar, Ibuprofen as an emerging organic contaminant in environment, distribution and remediation, Heliyon. 6 (2020) e04087, https://doi.org/10.1016/j.heliyon.2020.e04087.
[43] M. Schwientek, H. Rügner, S.B. Haderlein, W. Schulz, B. Wimmer, L. Engelbart, S. Bieger, C. Huhn, Glyphosate contamination in European rivers not from herbicide application? Water Res. 263 (2024) 122140 https://doi.org/10.1016/j.watres.2024.122140.
[44] A.F. Echeverri González, H. Zúñiga-Benítez, G.A. Peñuela, Removal of herbicide 2,4-D using constructed wetlands at pilot scale, Emerg. Contam. 5 (2019) 303–307, https://doi.org/10.1016/j.emcon.2019.09.001.
[45] R. Ranjan, S.P. Singh, Removal of urea and ammonia from wastewater, Energy, Environment, and Sustainability ((ENENSU)), pp 335–353, Springer.
[46] M. Burç, S. Köytepe, S. Titretir Duran, N. Ayhan, B. Aksoy, T. Seçkin, Development of voltammetric sensor based on polyimide-MWCNT composite membrane for rapid and highly sensitive detection of paracetamol, Measurement 151 (2020) 107103, https://doi.org/10.1016/j.measurement.2019.107103.
[47] W. Torres Pio dos Santos, E. Gledison Nascimento de Almeida, H. Eustáquio Alves Ferreira, D. Tofanello Gimenes, E. Mathias Richter, Simultaneous flow injection analysis of paracetamol and ascorbic acid with multiple pulse amperometric detection, Electroanalysis 20 (2008) 1878 – 1883. 10.1002/elan.200804262.
[48] Y.J. Shih, Z.L. Wu, S.K. Lin, Electrochemical detection of paracetamol using zeolitic imidazolate framework and graphene oxide derived zinc/nitrogen-doped carbon, Sens. Act. B. Chem. 409 (2024) 135600, https://doi.org/10.1016/j.snb.2024.135600.
[49] M.M. Barsan, C.T. Toledo, C.M.A. Brett, New electrode architectures based on poly (methylene green) and functionalized carbon nanotubes: Characterization and application to detection of acetaminophen and pyridoxine, J. Electroanal. Chem. 736 (2015) 8–15, https://doi.org/10.1016/j.jelechem.2014.10.026.
[50] A.U. Alam, Y. Qin, M.M.R. Howlader, N.X. Hu, M.J. Deen, Electrochemical sensing of acetaminophen using multi-walled carbonnanotube and -cyclodextrin, Sens. Act. B 254 (2018) 896–909, https://doi.org/10.1016/j.snb.2017.07.127.
[51] C.M. Teglia, F.A. Gutierrez, H.C. Goicoeche, Natural deep eutectic solvent: A novelty alternative as multi-walled carbon nanotubes dispersing agent for the determination of paracetamol in urine, Talanta 242 (2022) 123290, https://doi.org/10.1016/j.talanta.2022.123290.
[52] M. Vazan, J. Tashkhourian, B. Haghighi, A novel electrochemical sensor based on MoO_3 nanobelt-graphene oxide composite for the simultaneous determination of paracetamol and 4-aminophenol, Diam. Relat. Mater. 140 (2023) 110549, https://doi.org/10.1016/j.diamond.2023.110549 //.
[53] B.S. Sá, J.S. Stefano, L.R.G. Silva, T.M. Perfecto, T. Mazon, D.P. Volanti, B. C. Janegitz, C. Ribeiro, Methane-derived electrochemical sensor for determination of paracetamol and diquat, Mater. Chem. Phys. 315 (2024) 129025, https://doi.org/10.1016/j.matchemphys.2024.129025.
[54] S. Allende, Y. Liu, M.V. Jacob, Electrochemical sensing of paracetamol based on sugarcane bagasse-activated biochar, Ind. Crops Prod. 211 (2024) 118241, https://doi.org/10.1016/j.indcrop.2024.118241.
[55] M. Shahbakhsh, M. Noroozifar, Poly (dopamine quinone-chromium (III) complex) microspheres as new modifier for simultaneous determination of phenolic compounds, Biosens. Bioelectron. 102 (2018) 439–448, https://doi.org/10.1016/j.bios.2017.11.042.
[56] L.A. Goulart, R. Gonçalves, A.A. Correa, E.C. Pereira, L.H. Mascaro, Synergic effect of silver nanoparticles and carbon nanotubes on the simultaneous voltammetric determination of hydroquinone, catechol, bisphenol A and phenol, Microchim. Acta 185 (2018) 12, https://doi.org/10.1007/s00604-017-2540-5.
[57] F.A.A. Manan, W.W. Hong, J. Abdullah, N.A. Yusof, I. Ahmad, Nanocrystalline cellulose decorated quantum dots based tyrosinase biosensor for phenol determination, Mater. Sci. Eng. c. 99 (2019) 37–46, https://doi.org/10.1016/j.msec.2019.01.082.
[58] H. Hu, Y. Huang, Y. Yan, S.J. Hu, H.R. Liu, Wen, Simple synthesis of CeO_2 nanoparticle composites in situ grown on carbon nanotubes for phenol detection, Front. Chem. 10 (2022) 907777, https://doi.org/10.3389/fchem.2022.907777.
[59] M. Nurdin, M. Maulidiyah, A.H. Watoni, A. Armawans, L.O.A. Salim, Z. Arham, D. Wibowo, I. Irwan, A.A. Umar, Nanocomposite design of graphene modified TiO_2 for electrochemical sensing in phenol detection, Korean J. Chem. Eng. 39 (2022) 209–215, https://doi.org/10.1007/s11814-021-0938-6.
[60] I.K. Mhawi, S. Kaki, A. Babakhanian, Fabrication of PGE/CMC/Bathocuproine probe applicable for voltammetry determination of Phenol, J. App. Electrochem. (2024), https://doi.org/10.1007/s10800-024-02089-w.
[61] Z. Meng, M. Li, J. Shao, L. Yan, H. Yang, X. Liu, A sensitive electrochemical sensor based on the partial thermal decomposition of MIL-53(Fe) and reduced graphene oxide for phenol detection, Ionics 27 (2021) 4897–4906, https://doi.org/10.1007/s11581-021-04207-6.
[62] R. Wahab, F. Khan, N. Ahmad, M. Alam, Copper and iron based bimetallic nanocomposite: An enhanced and operative phenol sensor, Phys. E. 144 (2022) 11541, https://doi.org/10.1016/j.physe.2022.115419.
[63] R.D. Chio, F. Arena, S.G. Leonardi, K. Moulaee, G. Neri, N. Donato, Development of a MnO_2-modified screen-printed electrode for phenol monitoring, IEEE Trans. Instrum. Meas. 70 (2021), https://doi.org/10.1109/TIM.2020.3045808.